Phase Stability of Dynamically Disordered Solids from First Principles

Johan Klarbring* and Sergei I. Simak
Theoretical Physics Division, Department of Physics, Chemistry and Biology (IFM), Linköping University, SE-581 83, Linköping, Sweden

(Received 7 August 2018; published 28 November 2018)

Theoretical studies of phase stability in solid materials with dynamic disorder are challenging due to the failure of the standard picture of atoms vibrating around fixed equilibrium positions. Dynamically disordered solid materials show immense potential in applications. In particular, superionic conductors, where the disorder results in exceptionally high ionic conductivity, are very promising as solid state electrolytes in batteries and fuel cells. The biggest obstacle in living up to this potential is the limited stability of the dynamically disordered phases. Here, we outline a method to obtain the free energy of a dynamically disordered solid. It is based on a stress-strain thermodynamic integration on a deformation path between a mechanically stable ordered variant of the disordered phase, and the dynamically disordered phase itself. We show that the large entropy contribution associated with the dynamic disorder is captured in the behavior of the stress along the deformation path. We apply the method to Bi_2O_3, whose superionic δ phase is the fastest known solid oxide ion conductor. We accurately reproduce the experimental transition enthalpy and the critical temperature of the phase transition from the low temperature ground state α phase to the superionic δ phase. The method can be used for a first-principles description of the phase stability of superionic conductors and other materials with dynamic disorder, when the disordered phase can be connected to a stable phase through a continuous deformation path.

DOI: 10.1103/PhysRevLett.121.225702

The prediction of phase stability of dynamically disordered solid materials is a challenging problem for theoretical materials science. This is largely because these materials, despite displaying the characteristic time-averaged long range order of a crystalline solid, are not well described in the standard picture of atoms vibrating around fixed equilibrium positions. Clear examples include solids containing rotating molecular units and superionic conductors (superionics). Superionics are materials that, due to the dynamic disorder, have anomalously large ionic conductivities of up to $\sim 1\ \mathrm{S\,cm^{-1}}$ [1]. This makes them extremely suitable electrolytes for solid state batteries [2–5] and solid oxide fuel cells (SOFC) [6,7]. Recently, they have also shown promise in less obvious applications. For instance, as thermoelectrics, since their extremely anharmonic lattice vibrations provide ultralow thermal conductivity [8,9], and as mechanocaloric materials, since the superionic transition has a large associated entropy change and the transition temperature, T_c, can be tuned by an external stress field [10–12].

In most applications, the limited stability of the superionic phase prevents these materials from living up to their promise. The temperature range in which the superionic phase is stable typically begins above the operational temperature of the prospective application and is quite narrow. The temperature induced transformation to the superionic phase can either proceed as a discontinuous solid-solid phase transformation (type I superionic transition), where AgI is the prototypical example, or as a continuous increase in ionic conductivity within a preexisting phase (type II superionic transition), such as in fluorite structured materials, e.g., CaF_2 [1].

Dynamically disordered solids in general, and superionic phases in particular, are stabilized by the large entropy contribution associated with the dynamic disorder. This makes the prediction of their phase stability using computational methods very challenging, in particular for first-principles methods based on density functional theory (DFT). State-of-the-art first-principles predictions of phase stability typically rely on extracting free energies within a phonon picture. This can either be done using standard static phonon calculations, or using some phonon renormalization scheme. Such schemes require the existence of well-defined reference positions around which the atoms in the crystal thermally vibrate. This is clearly not the case for dynamically disordered mobile ions in superionic conductors. Thus, more advanced techniques, such as thermodynamic integration (TI) [13,14], are needed. TI techniques most commonly obtain the free energy of the real physical system by integrating from an artificial model system whose free energy is known. Such coupling constant integration (CCI) type techniques have recently been applied to study superionic water [15–18].

In this Letter we present an alternative TI-based route to obtain the free energy of a dynamically disordered solid. It relies on a DFT *ab initio* molecular dynamics (AIMD)

stress-strain TI between the dynamically disordered phase and a metastable ordered variant of the dynamically disordered phase. It has advantages over CCI techniques as it can connect two real phases, thus providing an upper bound to the free energy barrier separating the phases and explicitly revealing the entropy contribution that stabilizes the dynamically disordered phase over the ordered variant. To illustrate the method we chose the notoriously complex Bi_2O_3 system, whose superionic δ phase has the highest rate of ionic diffusion of all known solid oxides [7]. At ambient conditions Bi_2O_3 crystallizes in the monoclinic α phase, which transforms to the cubic superionic δ phase when heated above ~1003 K [19], which is stable up to the melting point of ~1100 K. On cooling from the δ phase, the system normally does not return directly to the α phase, but instead transforms into one of its metastable states. Most commonly to the tetragonal β phase at ~920 K and less often to the body centered cubic γ phase [19,20]. The β phase can be viewed as a closely related ordered variant of the superionic δ phase. A large body of experimental research has been directed towards attempting to stabilize δ-Bi_2O_3 at lower temperatures, while simultaneously retaining the high ionic conductivity, by methods including chemical doping [19,21,22], nanoconfinement [23], and thin film growth [24–26]. Several theoretical works have investigated the ionic diffusion in δ-Bi_2O_3 [27–29]. However, due to the difficulties of obtaining free energies of superionic phases mentioned above, no first-principles theoretical description of the phase stability exists to date, leaving any attempt at stabilizing δ-Bi_2O_3 without a firm physical foundation. We perform a stress-strain TI between the ordered metastable β phase and the disordered superionic δ phase of Bi_2O_3. We explicitly show that the stabilizing entropy of the superionic δ phase is seen in the behavior of the stress tensor on a deformation path between the two phases. We further calculate the free energies of the ordered α and β phases in the temperature dependent effective potential (TDEP) [30,31] phonon picture. The α- to δ-phase transition is accurately reproduced, with both the temperature and the enthalpy of the transition matching experiments very well.

All DFT calculations were performed in the framework of the projector augmented wave (PAW) [32] method using the Vienna *ab initio* simulation package (VASP) [33–35]. Exchange-correlation effects were treated using the PBEsol [36] form of the generalized gradient approximation (GGA). The Kohn-Sham orbitals were expanded in plane waves with a kinetic energy cutoff of 600 eV. Supercells of 160 atoms for the α phase and 240 atoms for the β and δ phases were used. For these large supercells Γ-point sampling of the Brillouin zone was found to be sufficient to provide high accuracy of the TI. The convergence criterion for the electronic self-consistent iterations was set to 10^{-6} eV. Born-Oppenheimer (BO) AIMD simulations were performed in the canonical (*NVT*) ensemble. The temperature was controlled by a Nosé-Hoover thermostat using the default Nosé mass parameter as set by VASP and a 2 fs time step. The temperature dependence of all equilibrium lattice parameters was obtained from a set of AIMD runs where the lattice parameters were iteratively changed until the converged values of all components of the Cauchy stress tensor, $\boldsymbol{\sigma}$, were < 1 kBar.

Temperature dependent phonon dispersions and free energies of the ordered α and β phases were obtained using the TDEP method [30,31]. TDEP uses forces and atomic displacements from AIMD to construct the harmonic potential that best reproduces the true BO energy surface (see Supplemental Material [37] for details).

Quite generally for a rotationally invariant crystal, the differential of the Helmholtz free energy, $F = U - TS$, where U is the internal energy, T the temperature, and S the entropy, can be written as [38,39]

$$dF(\{\mathbf{X}, \boldsymbol{\eta}\}, T) = -SdT + V(\mathbf{X})\boldsymbol{\tau} : d\boldsymbol{\eta}. \tag{1}$$

Here, $V(\mathbf{X})$ is the volume of an (arbitrary) reference configuration $\mathbf{X}$, $\boldsymbol{\eta}$ is the Lagrangian strain tensor, defined with respect to $\mathbf{X}$, and $\boldsymbol{\tau}$ is the thermodynamic, or second Piola-Kirchoff (PK2) stress tensor. The operation ":" is a contraction over both indices, i.e., $\boldsymbol{\tau} : d\boldsymbol{\eta} = \sum_{i,j} \tau_{ij} d\eta_{ij}$. From DFT based AIMD, we have access to the Cauchy stress tensor $\boldsymbol{\sigma}$, which is related to the PK2 stress as $\boldsymbol{\tau} = J\boldsymbol{\alpha}^{-1}\boldsymbol{\sigma}\boldsymbol{\alpha}^{-T}$, where $\boldsymbol{\alpha}$ is the deformation gradient and $J = \det(\boldsymbol{\alpha})$ (see Supplemental Material [37] for the details).

Equation (1) can be integrated at constant T to yield the free energy difference, ΔF, between the reference configuration $\mathbf{X}$, described by a tensor $\boldsymbol{h}(\boldsymbol{X})$ defining the supercell used in AIMD, and a configuration $\mathbf{x}$ described by $\boldsymbol{h}(\boldsymbol{x}) = \boldsymbol{\alpha}\boldsymbol{h}(\boldsymbol{X})$. The general expression for a deformation path parametrized by λ is derived in the Supplemental Material [37] and reads

$$\Delta F(\lambda) = \int_0^\lambda V(\lambda')\boldsymbol{\sigma}(\lambda')\boldsymbol{h}^{-T}(\lambda') : \frac{\partial \boldsymbol{h}(\lambda')}{\partial \lambda'} d\lambda'. \tag{2}$$

In the special case of interest for our present purposes, $\boldsymbol{h}(\lambda)$ is diagonal and we use a linear interpolation between the reference ($\boldsymbol{h}^0$) and final ($\boldsymbol{h}^1$) configurations, i.e., $\boldsymbol{h}(\lambda) = \boldsymbol{h}^0 + \lambda(\boldsymbol{h}^1 - \boldsymbol{h}^0)$. In this case, Eq. (2) reduces to

$$\Delta F(\lambda) = \int_0^\lambda V(\lambda') \sum_i \sigma_{ii}(\lambda') \frac{h^1_{ii} - h^0_{ii}}{h_{ii}(\lambda')} d\lambda'. \tag{3}$$

Practical use of Eq. (3) entails performing AIMD at a series of configurations $\boldsymbol{h}(\lambda)$ to obtain corresponding $\boldsymbol{\sigma}(\lambda)$ and numerically evaluating the integral.

We note that the stress-strain TIs of Refs. [40,41] have relied on formulas that are simplified special cases of Eq. (2) and Haskins *et al.* [42] have, in an entirely different way, derived the same general expression to study the phase

stability in NiTi. Importantly, all the transitions investigated with help of stress-strain TIs have so far been between ordered structures. We will show how the stress-strain TI can be used to study the transition between an ordered and a heavily disordered phase.

The tetragonal unit cell of β-Bi_2O_3 can be transformed into a representation of the cubic δ phase by compressing the c axis and expanding the a and b axes to a state of zero stress with $a/c = \sqrt{2}$. Since the lattice parameters of the two phases are quite close, we perform the integration of Eq. (3) in two steps; i.e., we write $\Delta F_{\beta\to\delta} = \Delta F_1 + \Delta F_2$, where the first term corresponds to the free energy change when compressing the c axis and the second term to the change upon subsequent expansion of a and b.

A noticeable complication of the stress-strain TI is the fact that the β phase is ordered, while the oxygen sublattice is heavily disordered in the δ phase. We should thus expect that this disordering will set in somewhere along the integration path. Careful consideration needs to be made to ensure that thermodynamic equilibrium is reached at each point along the path and that the stress along the path is integrable. This would not be an issue given infinite simulation time. In practice, however, this is a potential problem since very long simulation times may be required to capture the transition from order to disorder. To address this issue we note that since the disorder is mediated by oxide ion diffusion, we expect it to be promoted by expansion and conversely, to some degree, suppressed by contraction of the lattice. With these considerations in mind we proceed with the TI for Bi_2O_3 at 900 K in the following way. We initially run ~40 ps AIMD simulations for 4 structures with the c axis varying between its values in the β and δ phases, parametrized by λ_1. This produces an expected approximately linear decrease in σ_{33} [43], and a corresponding quadratic increase in the free energy, as shown in Fig. 1. During these simulations the O sublattice remains ordered.

We then start to expand the a and b axes towards the δ phase, this second path is parametrized by λ_2. On the first point along this expansion an AIMD simulation is run for ~150 ps. During this time, substantial disordering of the O sublattice is observed, starting from around ~35 ps into the simulation. Correspondingly, there is a large nonzero slope of the O mean square displacement (MSD). The averaging of the stress tensor is calculated starting from the AIMD time step where a continuous rate of diffusion of the O ions is observed; this is identified by a linear behavior of the MSD as a function of time, see Supplemental Material [37] for more details. Importantly, this disordering of the O sublattice can be seen through the behavior of the stress. Indeed, we find a decrease of σ_{11} and σ_{22}, rather than the expected increase, upon expanding the a and b axes, explicitly due to the O sublattice disorder (see Fig. 1). This can be understood as follows: Once the system is distorted far enough away from the ordered β phase,

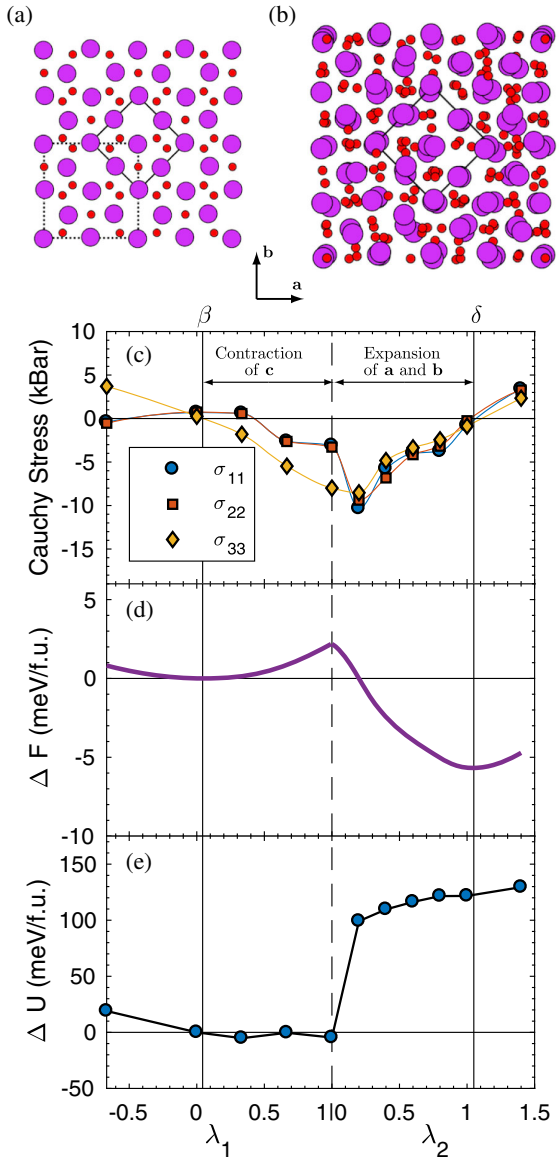

FIG. 1. Bi_2O_3 at 900 K. (a) The $2 \times 2 \times 2$ supercell of β-Bi_2O_3 used in this work. The dashed lines show the primitive unit cell. The solid black lines show the relation to the conventional fluorite unit cell of δ-Bi_2O_3. (b) Snapshot of atomic positions in the heavily disordered superionic δ phase. (c) Diagonal components of the Cauchy stress tensor $\boldsymbol{\sigma}$ on the deformation path between the β and the δ phase. (d) Free energy and (e) internal energy difference with respect to the β phase along the deformation path.

entropic effects make a disorder among the O ions, mediated by diffusion, thermodynamically preferable. The diffusion is, in turn, promoted by lattice expansion, which means that the structure can lower its free energy by expanding in order to further increase the disorder among the O ions. A snapshot (atomic positions and velocities) from this simulation, after the disorder has sat in, is then used as initial structures for the subsequent simulations. Four more simulations are performed with progressively expanded a and b, with the final simulation corresponding

to their values in the δ phase. All three diagonal components of the stress tensor are found to continuously increase toward zero with increasing a and b, admitting values within 1 kBar of 0 at the lattice parameters corresponding to the δ phase. This produces a corresponding decrease of the free energy, with an extremum in the δ phase. Two additional simulations with $\lambda_1 < 0$ and $\lambda_2 > 1$ were finally performed to reveal that both the β and δ phases are real free energy minima along the path, see Fig. 1.

Finally, to make sure that the O sublattice disorder does not in fact set in earlier along the path, we performed another ~110 ps of AIMD for the point corresponding to $\lambda_1 = 1$. During the total ~150 ps of simulation time only a couple of O ions are displaced from their positions in the β phase, i.e., no continuous diffusion, and the displacement of these O ions has essentially zero effect on the stresses.

In the end, we find that the δ-Bi_2O_3 is ~6 meV/f.u. more stable than β-Bi_2O_3 at 900 K, with a very small upper bound to the free energy barrier of ~2 meV/f.u.

We explicitly point out the important finding that the entropic stabilization mechanism of a dynamically disordered solid can be seen through the behavior of the stress tensor on a deformation path from an ordered phase towards the disordered phase. We see in Fig. 1(e) that at the point where the disorder sets in, there is a corresponding large increase in U, since the system is breaking out of its low energy ordering. However, there is a simultaneous decrease in F, due to the behavior of the stress, indicating an even larger increase in entropy. Indeed, the β phase is ~120 meV/f.u. lower in energy than the δ phase at 900 K. This leaves an entropy difference of $T\Delta S \approx 126$ meV/f.u. between the β and δ phase, to make up the ~6 meV/f.u. free energy difference in favor of the δ phase at this temperature.

We now use the TDEP method to obtain the free energies of the ordered α and β phases. The usage of TDEP is crucial since β-Bi_2O_3 is dynamically unstable in a (quasi)harmonic description [44]. The free energy difference is shown by the blue circles in Fig. 2. At 300 K α is ~150 meV/f.u. more stable than β. This free energy difference is reduced to only ~22 meV/f.u. at 900 K. At temperatures starting from 1050 K the O ions do not stay around their ideal positions in the β phase but instead show substantial diffusion during the simulation, indicating a spontaneous transformation toward the disordered δ phase. This indicates that the free energy barrier between β and δ (as seen at 900 K in Fig. 1) disappears somewhere between 900 and 1050 K, which effectively makes the β phase dynamically unstable.

Combining the TDEP results and the stress-strain TI (Fig. 1) at 900 K indicates that the α phase is favored by ~14 meV/f.u. compared to the δ phase. In order to obtain the temperature dependence of the free energy of the δ phase we use the standard expression

$$\frac{F(\mathbf{x},T)}{T} - \frac{F(\mathbf{x},T_{\mathrm{ref}})}{T_{\mathrm{ref}}} = -\int_{T_{\mathrm{ref}}}^{T} \frac{U(T')}{T'^2}\, dT', \qquad (4)$$

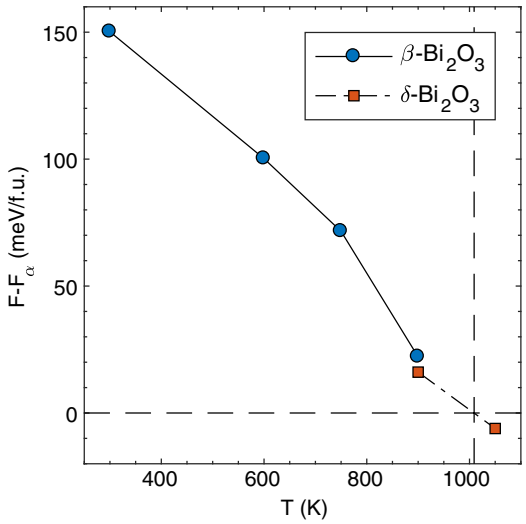

FIG. 2. Free energy difference of the β phase (blue circles) and δ phase (red squares) with respect to the α phase, obtained as described in the text. The vertical line shows the temperature of the α-δ transition.

where T_{ref} is some reference temperature (details are provided in the Supplemental Material [37]).

The red squares in Fig. 2 give the obtained free energy difference between the α and the δ phase. At 1050 K it is ~8 meV/f.u. in favor of the δ phase and the obtained transition temperature (the vertical line in Fig. 2) of the α to δ transition, $T_{\alpha-\delta} \approx 1010$ K, is in excellent agreement with the experimental value of ~1003 K. This close agreement may look fortuitous considering the approximations employed in our simulations, which include the approximate exchange-correlation treatment in DFT and the finite-sized and defect-free supercells used in the AIMD simulations. However, further validation of the results can be obtained by investigating the transition enthalpy of the α to δ transition, given by the difference in the internal energies of the α and δ phase at $T_{\alpha-\delta}$. Our calculated transition enthalpy is ~0.32 eV/f.u., which agrees very well with the experimental value of ~0.31 eV/f.u. [20]. This is very large for a solid-solid transition, which is a direct result of the very high entropy associated with the extreme disorder among the O ions in the superionic δ phase. The fact that our calculated transition enthalpy and transition temperature agrees with the experimental values shows that we capture the violent energy-entropy competition that governs the phase stability of dynamically disordered solids, and we view this as a strong indicator of the validity of the present method.

Let us briefly discuss the place of the β phase in the polymorphism of Bi_2O_3. Experimentally, the δ phase is found to always persist to temperatures below $T_{\alpha-\delta}$ when cooling. The transformation into the β phase occurs at ~80 K below $T_{\alpha-\delta}$. Figure 1(d) shows that the free energy barrier between β and δ is very small. Since the α-δ (and α-β) barrier

is very likely much larger, the system will fall into the β free energy minimum when cooling from δ. Upon further cooling the system eventually returns to the α phase.

Finally, we point out that the stress-strain TI between the β and δ phase can be straightforwardly applied also to doped Bi_2O_3. The relative stability of the β and δ phases at different dopant concentrations of e.g., Tm [21] appears to be the crucial factor in stabilizing the δ phase at low temperatures. The application of the present method may thus provide important physical insight, which could be essential in designing new Bi_2O_3 based solid electrolytes.

In summary, we have outlined a method to obtain the free energy of a dynamically disordered solid. The method is based on a stress-strain TI from an ordered variant of the disordered phase. We have shown that the stabilizing entropy associated with the dynamic disorder is captured in the behavior of the stress. Free energies of other ordered polymorphs are obtained using the TDEP method. We have applied this method to the superionic oxide Bi_2O_3. The transition from the low temperature ordered α phase into the highly disordered superionic δ phase is accurately reproduced, with both the temperature and the enthalpy of the transition in excellent agreement with experiment. The method can be applied to study the phase stability of materials containing large degrees of dynamic disorder where the disordered phase can be connected to an ordered (real or artificial) stable system through a continuous deformation path.

The support from the Swedish Research Council (VR) (Project No. 2014-4750), and the Swedish Government Strategic Research Area in Materials Science on Functional Materials at Linköping University (Faculty Grant SFO-Mat-LiU No. 2009 00971) are acknowledged by S. I. S and J. K. The computations were performed on resources provided by the Swedish National Infrastructure for Computing (SNIC) at the PDC Centre for High Performance Computing (PDC-HPC), the National Supercomputer Center (NSC).

*johan.klarbring@liu.se

[1] S. Hull, Rep. Prog. Phys. **67**, 1233 (2004).
[2] Y. Wang, W. D. Richards, S. P. Ong, L. J. Miara, J. C. Kim, Y. Mo, and G. Ceder, Nat. Mater. **14**, 1026 (2015).
[3] N. Kamaya, K. Homma, Y. Yamakawa, M. Hirayama, R. Kanno, M. Yonemura, T. Kamiyama, Y. Kato, S. Hama, K. Kawamoto, and A. Mitsui, Nat. Mater. **10**, 682 (2011).
[4] H. Fang and P. Jena, Proc. Natl. Acad. Sci. U.S.A. **114**, 11046 (2017).
[5] M. H. Braga, J. A. Ferreira, A. J. Murchison, and J. B. Goodenough, J. Electrochem. Soc. **164**, A207 (2017).
[6] J. A. Kilner and M. Burriel, Annu. Rev. Mater. Res. **44**, 365 (2014).
[7] E. D. Wachsman and K. T. Lee, Science **334**, 935 (2011).
[8] H. Liu, X. Shi, F. Xu, L. Zhang, W. Zhang, L. Chen, Q. Li, C. Uher, T. Day, and G. J. Snyder, Nat. Mater. **11**, 422 (2012).
[9] D. J. Voneshen, H. C. Walker, K. Refson, and J. P. Goff, Phys. Rev. Lett. **118**, 145901 (2017).
[10] C. Cazorla and D. Errandonea, Nano Lett. **16**, 3124 (2016).
[11] A. K. Sagotra, D. Errandonea, and C. Cazorla, Nat. Commun. **8**, 963 (2017).
[12] A. Aznar, P. Lloveras, M. Romanini, M. Barrio, J.-L. Tamarit, C. Cazorla, D. Errandonea, N. D. Mathur, A. Planes, X. Moya, and L. Mañosa, Nat. Commun. **8**, 1851 (2017).
[13] M. Tuckerman, *Statistical Mechanics: Theory and Molecular Simulation* (Oxford University Press, Oxford, England, 2010).
[14] D. Alfè, G. D. Price, and M. J. Gillan, Phys. Rev. B **64**, 045123 (2001).
[15] M. A. Morales, E. Schwegler, D. Ceperley, C. Pierleoni, S. Hamel, and K. Caspersen, Proc. Natl. Acad. Sci. U.S.A. **106**, 1324 (2009).
[16] H. F. Wilson and B. Militzer, Phys. Rev. Lett. **104**, 121101 (2010).
[17] H. F. Wilson and B. Militzer, Phys. Rev. Lett. **108**, 111101 (2012).
[18] H. F. Wilson, M. L. Wong, and B. Militzer, Phys. Rev. Lett. **110**, 151102 (2013).
[19] M. Drache, P. Roussel, and J.-P. Wignacourt, Chem. Rev. **107**, 80 (2007).
[20] H. Harwig and A. Gerards, Thermochim. Acta **28**, 121 (1979).
[21] A. Dapčević, D. Poleti, J. Rogan, A. Radojković, M. Radović, and G. Branković, Solid State Ionics **280**, 18 (2015).
[22] K. Shitara, T. Moriasa, A. Sumitani, A. Seko, H. Hayashi, Y. Koyama, R. Huang, D. Han, H. Moriwake, and I. Tanaka, Chem. Mater. **29**, 3763 (2017).
[23] S. Sanna, V. Esposito, J. W. Andreasen, J. Hjelm, W. Zhang, T. Kasama, S. B. Simonsen, M. Christensen, S. Linderoth, and N. Pryds, Nat. Mater. **14**, 500 (2015).
[24] N. V. Skorodumova, A. K. Jonsson, M. Herranen, M. Strömme, G. A. Niklasson, B. Johansson, and S. I. Simak, Appl. Phys. Lett. **86**, 241910 (2005).
[25] P. L. Popa, S. Sønderby, S. Kerdsongpanya, J. Lu, N. Bonanos, and P. Eklund, J. Appl. Phys. **113**, 046101 (2013).
[26] P. L. Popa, S. Sønderby, S. Kerdsongpanya, J. Lu, H. Arwin, and P. Eklund, Thin Solid Films **624**, 41 (2017).
[27] C. E. Mohn, S. Stølen, S. T. Norberg, and S. Hull, Phys. Rev. Lett. **102**, 155502 (2009).
[28] C. E. Mohn, S. Stølen, S. T. Norberg, and S. Hull, Phys. Rev. B **80**, 024205 (2009).
[29] A. Seko, Y. Koyama, A. Matsumoto, and I. Tanaka, J. Phys. Condens. Matter **24**, 475402 (2012).
[30] O. Hellman, I. A. Abrikosov, and S. I. Simak, Phys. Rev. B **84**, 180301 (2011).
[31] O. Hellman, P. Steneteg, I. A. Abrikosov, and S. I. Simak, Phys. Rev. B **87**, 104111 (2013).
[32] P. E. Blöchl, Phys. Rev. B **50**, 17953 (1994).
[33] G. Kresse and J. Furthmüller, Comput. Mater. Sci. **6**, 15 (1996).
[34] G. Kresse and J. Furthmüller, Phys. Rev. B **54**, 11169 (1996).
[35] G. Kresse and D. Joubert, Phys. Rev. B **59**, 1758 (1999).

[36] J. P. Perdew, A. Ruzsinszky, G. I. Csonka, O. A. Vydrov, G. E. Scuseria, L. A. Constantin, X. Zhou, and K. Burke, Phys. Rev. Lett. **100**, 136406 (2008).
[37] See Supplemental Material at http://link.aps.org/supplemental/10.1103/PhysRevLett.121.225702 for derivation of Eqs. (2) and (3), examples of TDEP phonon dispersion, and details of the thermodynamic integration.
[38] D. C. Wallace, *Thermodynamics of Crystals* (Dover Publications, New York, 1998).
[39] D. C. Wallace, Solid State Phys. **25**, 301 (1970).
[40] V. Ozolins, Phys. Rev. Lett. **102**, 065702 (2009).
[41] C. Cazorla, D. Alfè, and M. J. Gillan, Phys. Rev. B **85**, 064113 (2012).
[42] J. B. Haskins, A. E. Thompson, and J. W. Lawson, Phys. Rev. B **94**, 214110 (2016).
[43] We follow the sign convention where a positive diagonal stress component indicates that the crystal is in a state of expansion.
[44] A. L. J. Pereira, O. Gomis, J. A. Sans, J. Contreras-García, F. J. Manjón, P. Rodríguez-Hernández, A. Muñoz, and A. Beltrán, Phys. Rev. B **93**, 224111 (2016).